energies

MDPI

Article

Measuring Interparticle Friction of Granules for Micromechanical Modeling

Yuan Li [1,2], Dave Chan [1,3] and Alireza Nouri [1,*]

[1] Department of Civil and Environmental Engineering, School of Mining and Petroleum Engineering, University of Alberta, Edmonton, AB T6G 1H9, Canada; yuan16@ualberta.ca (Y.L.); dave.chan@ualberta.ca (D.C.)
[2] Thurber Engineering Ltd., 4127 Roper Road NW, Edmonton, AB T6B 3S5, Canada
[3] College of Civil Engineering and Architecture, China Three Gorges University, Yichang 443002, China
* Correspondence: anouri@ualberta.ca

Abstract: The aim of this paper is to develop an experimental procedure to measure contact friction between granular particles. The contact friction is a micro-property needed in the micromechanical modeling of a granular medium. The proposed method can measure the interparticle friction of idealized spherical particles using the conventional direct shear apparatus in soil testing. In preparation for the test, the test specimen is made of four steel balls embedded halfway in a sulfaset paste plate positioned in a statically determinant configuration to provide point contacts among the steel balls. The upper half of the shear box contains one steel ball, which is supported by three steel balls in the lower shear box, ensuring contact points at all times during the test. Shear force and shear displacement are measured under a specific normal force during the test. An analytical equation is developed based on the geometrical configuration of the balls to calculate the interparticle friction angle. The test is shown to be repeatable, and the calculated interparticle friction angle agrees well with experimental measurements with a high degree of accuracy and consistency.

Keywords: interparticle friction; spherical particle shear test; direct shear test; friction of steel ball; granular friction

Citation: Li, Y.; Chan, D.; Nouri, A. Measuring Interparticle Friction of Granules for Micromechanical Modeling. *Energies* **2022**, *15*, 3967. https://doi.org/10.3390/en15113967

Academic Editor: Mofazzal Hossain

Received: 19 April 2022
Accepted: 25 May 2022
Published: 27 May 2022

1. Introduction

The aim of this paper to develop a laboratory testing method to measure the contact friction between granular particles. The contact friction is a micro-property that is needed in micromechanical modeling of a granular medium, such as modeling sand production in oil wells. Oil extraction from sandstone reservoirs is usually carried out with an oil well equipped with a wellbore screen. During oil flow, sand particles are mixed with the oil going through the screen and lifting system. The process of producing sand from oil extraction is called sand production. Depending on the relative sizes between the sand particles and the screen openings, particles may jam the opening, which causes a reduction in oil flow. Additionally, excessive sand production leads to abrasion of the pipes, pumps, and other components of the production system, which increases maintenance costs. The flow of sand particles depends on the friction of the material. To study sand production, micromechanical modeling has been used. To model sand particles individually, it is necessary to determine the contact friction of the particles.

Micromechanics modeling is emerging as a popular technique in geotechnical analysis. The method provides an in-depth understanding of the deformation and failure processes at the microscopic level of granular material. Micromechanical analysis has become more widely used by geotechnical engineers due to the advancement of computer capacities and numerical methods. Therefore, micromechanical parameters of granular material are needed to carry out micromechanics analysis. The interparticle friction angle is one of the most important parameters in micromechanical modeling.

Many apparatuses have been developed to measure the interparticle friction angle of granular particles [1–8]. Ecke et al. [4] developed an apparatus based on the principle of atomic force microscope (AFM) to measure the normal and shear forces acting between a particle and another solid surface. Jones [9] reported the results of friction tests performed with AFM on artificial particles, the sizes of which varied between 6 µm and 0.20 mm, and mentioned that AFM measurements might be less useful for large particles and large normal contact force situations. Furthermore, Tyrrel and Cleaver [3] developed an instrument to measure interparticle forces with AFM technology with a discussion on instrument calibrations. They pointed out that calibration errors and non-repeatability in the stiffness of the cantilever arm of the AFM device can affect the precision of measurements by 30% or more. Cavarretta et al. [5] developed a robust apparatus to measure the friction between two particles of coarse sand sizes (0.2–2.0 mm) immersed in a fluid. However, this apparatus is limited to testing coarser sands with regular shapes. Besides, the fluid used for immersion is subject to atmospheric pressure, and the ambient relative humidity cannot be controlled, which can significantly affect the measurements for smoother particles.

Senetakis and Coop [6] developed an apparatus to perform interparticle shearing tests at very small displacements. Tests on chrome steel balls and quartz particles demonstrated high repeatability of the results. However, the particles must have a relatively convex shape, and the size of the particles is limited to between about 0.50 and 5.0 mm. Additionally, the particles have to be reasonably symmetrical about the axis of shearing to avoid significant lateral forces in the out-of-plane horizontal direction during sliding. This apparatus was later upgraded and used to study the effect of shearing velocity on the interparticle behavior of granular and composite materials [8] and the micro-slip displacement of geological materials [7]. Experiments on pairs of grains, including natural and idealized grains, of about 1.0–5.0 mm in diameter were conducted. Superglue was used to secure the grains on the mounts, and the normal force applied was in the range of 1 to 8 N. Sandeep and Senetakis [10] also developed a large-size apparatus with the capability to measure friction between fine spherical gravel and ballast. Although the test results of the above apparatuses are shown to be reproducible, the alignment of grains is critical as that may affect the results. In general, direct measurement of interparticle contact friction is challenging, and it is not often carried out commercially due to the limited availability of sophisticated equipment and a lack of experience and expertise.

To eliminate the heterogeneities that occur in natural materials and ensure the reproducibility of the test results, idealized spherical particles (e.g., glass beads and steel balls) are widely used in the laboratory to study the mechanical properties of cemented or uncemented granular material [11–15].

The discrete element method (DEM) simulates the macro behavior of a granular system based on the interaction and movement of the individual particles, which includes cemented granular material. The particle flow code (PFC), as one of the DEM programs, has been used with increasing popularity to model natural or artificial cemented granular material [13,16–20]. PFC can model the movement and interaction of 2D circular particles (or 3D spherical particles) in a cemented material by bonding the particles to their neighbors. Moreover, the solid medium can be represented by the assembly of circular discs (2D) or spheres (3D) in PFC with a set of micromechanical properties at the particle contact. Therefore, it is important to determine the micro-parameters, such as interparticle friction, that will result in the appropriate macro-mechanical responses.

To determine the interparticle friction, while building a new apparatus is costly and time-consuming, a simple and effective method is developed in this study to measure the interparticle friction angle of spherical particles using a conventional direct shear apparatus.

2. Specimen Preparation

To develop an analytical solution to calculate contact friction, round spheres are used due to geometric simplicity. However, the same procedure and calculation method can be

used for irregular particles. In this work, steel balls of 1 inch in diameter were used for preparing the specimens for the direct shear tests.

As shown in Figure 1a, a steel ball (Ball A) is set in the sulfaset paste plate to fit in the upper shear box and rest on top of the bottom half in point contacts with the steel balls in the lower half of the shear box. The bottom half of the shear box (about 58 × 58 mm in size) contains three 1-inch diameter steel balls (Balls B, C, and D), embedded in the center of a sulfaset paste plate. All three steel balls are held in place to ensure contact with each other, and the sulfaset paste is poured into the shear box mold above the mid-height of the ball to provide strong bonding. In addition, the steel balls are glued to the paste plate to prevent rolling. The direct shear apparatus used for the interparticle friction measurement is shown in Figure 1b. Each test was repeated once to examine reproducibility under normal loads of 60, 100, and 200 N.

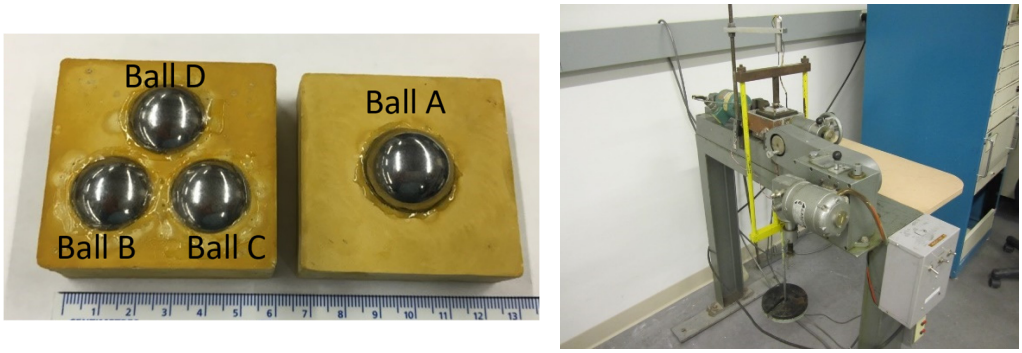

(**a**) (**b**)

Figure 1. (**a**) The embedded steel balls in the sulfaset paste plate for interparticle friction measurement. (**b**) The direct shear apparatus used for interparticle friction measurement.

3. Geometry and Mechanical Analysis

As shown in Figure 2, points B, C, and D represent the centers of the steel balls in the bottom half of the shear box. Point A represents the center of the steel ball in the upper half of the shear box, and point A_{xy} is the projection of point A on the xy plane. In the beginning of the test, Ball A is positioned at the center of the bottom shear box, and it is in contact with Balls B, C, and D.

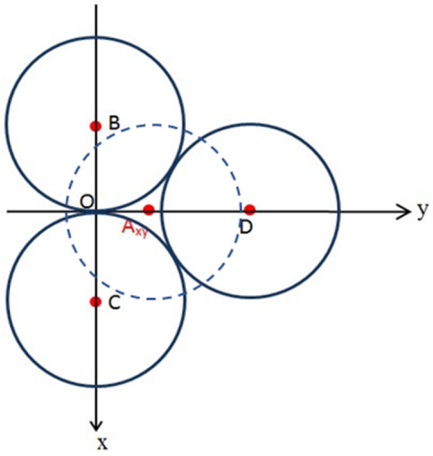

Figure 2. The projection of the steel balls B, C, and D in the lower shear box on the xy plane. The centers of balls A, B, C, and D are shown in red dots.

During the test, a constant displacement rate of 0.005 mm/s was applied on the lower shear box, and Ball A would ride over Balls B and C. Based on the geometry and mechanical relationships among the steel balls, the interparticle friction angle can be calculated from

the measured horizontal force and the applied normal force. The analytical equation to calculate the friction between the ball contact surfaces is derived below.

The rectangular Cartesian coordinate system is used, as shown in Figure 3. At any instance, during the movement of Balls B and C relative to Ball A, all the applied forces on Ball A should satisfy equilibrium (momentary), assuming a quasi-static condition and neglecting inertia effects. Ball A is subjected to the external force F, contact force F_a at contact point a between Balls A and B, and contact force F_b at contact point b between steel Balls A and C. Gravitational force is neglected since it is small compared to the applied normal and shear forces.

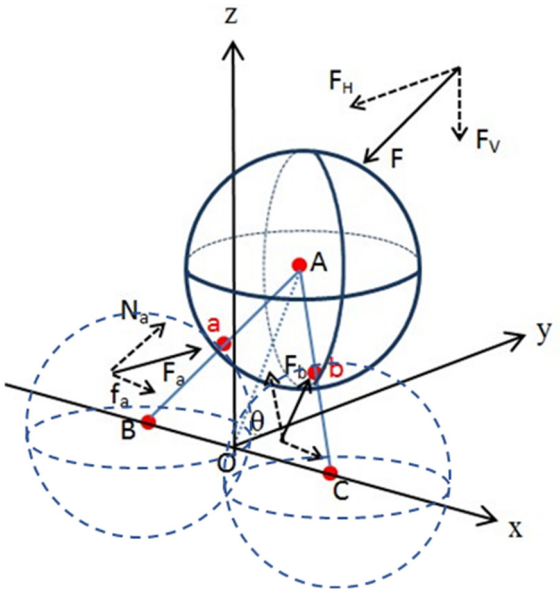

Figure 3. The applied forces on Ball A in the upper shear box in contact with Balls B and C at contact points a and b, respectively.

The external force F has two components: the vertical force, F_v, and the horizontal force, F_H. In the direct shear test, the vertical force, F_v, is equal to the applied normal force, and the horizontal force, F_H, is the measured shear force in the horizontal direction. The contact force F_a is the resultant force of the local normal force N_a and the friction force f_a at contact point a. Similarly, the force F_b can be divided into the local normal force N_b and the friction force f_b at contact point b. Since there are only three forces applied on Ball A, these three forces must be concentric.

The external vertical force and horizontal force can be expressed as:

$$\left\{ \begin{array}{l} \vec{F_v} = 0\hat{i} + 0\hat{j} - F_v\hat{k} \\ \vec{F_H} = 0\hat{i} - F_H\hat{j} - 0\hat{k} \end{array} \right\} \quad (1)$$

and the external resultant force F is:

$$\vec{F} = 0\hat{i} - F_H\hat{j} - F_v\hat{k} \quad (2)$$

The motion of the center of Ball A and contact points a and b are shown in Figure 4. Let r be the radius of the steel ball and θ denotes the angle between line AO and the xy plane, then the coordinates of all the points are given by:

$$\begin{cases} O = (0,\ 0,\ 0) \\ A = \left(0,\ \sqrt{3}r\cos\theta,\ \sqrt{3}r\sin\theta\right) \\ B = (-r,\ 0,\ 0) \\ C = (r,\ 0,\ 0) \\ a = \left(-\frac{r}{2},\ \frac{\sqrt{3}}{2}r\cos\theta,\ \frac{\sqrt{3}}{2}r\sin\theta\right) \\ b = \left(\frac{r}{2},\ \frac{\sqrt{3}}{2}r\cos\theta,\ \frac{\sqrt{3}}{2}r\sin\theta\right) \end{cases} \tag{3}$$

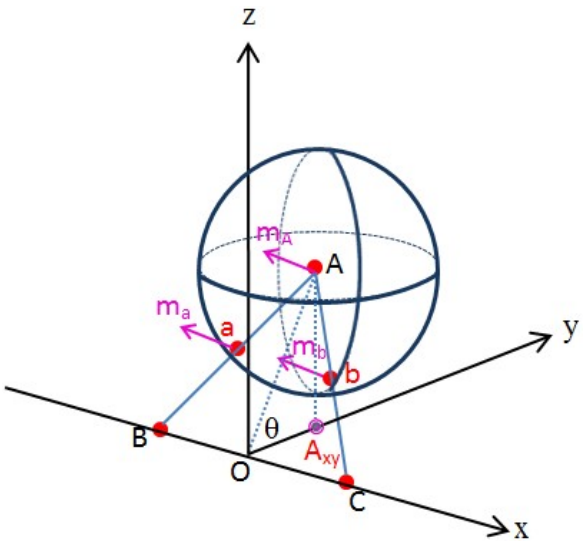

Figure 4. Motion of Ball A in the upper shear box against Balls B and C. m_A, m_a and m_b are movement vectors at Point A (Ball A center), and contact points a and b.

Therefore, the unit vectors, along the BA and CA directions, can be written as:

$$\begin{cases} \vec{u_{BA}} = \frac{\vec{BA}}{\left|\vec{BA}\right|} = \frac{1}{2}\hat{i} + \frac{\sqrt{3}}{2}\cos\theta\hat{j} + \frac{\sqrt{3}}{2}\sin\theta\hat{k} \\ \vec{u_{CA}} = \frac{\vec{CA}}{\left|\vec{CA}\right|} = -\frac{1}{2}\hat{i} + \frac{\sqrt{3}}{2}\cos\theta\hat{j} + \frac{\sqrt{3}}{2}\sin\theta\hat{k} \end{cases} \tag{4}$$

Since the movement vector at point A is equal to:

$$\vec{m_A} = 0\hat{i} - \sqrt{3}r\sin\theta\hat{j} + \sqrt{3}r\cos\theta\hat{k} \tag{5}$$

the unit vector in the direction of movement of Ball A can be determined from:

$$\vec{u_{m_A}} = \vec{u_{m_a}} = \vec{u_{m_b}} = \frac{\vec{m_A}}{\left|\vec{m_A}\right|} = -\sin\theta\hat{j} + \cos\theta\hat{k} \tag{6}$$

Let N and f be the magnitudes of the local normal force and friction force at contact point a, respectively, then the normal force and friction force applied to steel Ball A at contact point a can be calculated from:

$$\begin{cases} \vec{N_a} = N * \vec{u_{BA}} = N * \left(\frac{1}{2}\hat{i} + \frac{\sqrt{3}}{2}\cos\theta\hat{j} + \frac{\sqrt{3}}{2}\sin\theta\hat{k}\right) \\ \vec{f_a} = f * \left(-\vec{u_{m_a}}\right) = f * \left(\sin\theta\hat{j} - \cos\theta\hat{k}\right) \end{cases} \tag{7}$$

Hence, the contact force F_a at contact point a is equal to:

$$\vec{F_a} = \vec{N_a} + \vec{f_a} = \frac{1}{2}N\hat{i} + \left(\frac{\sqrt{3}}{2}N\cos\theta + f\sin\theta\right)\hat{j} + \left(\frac{\sqrt{3}}{2}N\sin\theta - f\cos\theta\right)\hat{k} \tag{8}$$

Since Balls B and C are symmetrical about the Y axis, the magnitudes of the local normal force and friction force at contact point a should be the same as those at contact point b. Similarly, the contact force F_b at contact point b is given by:

$$\vec{F_b} = \vec{N_b} + \vec{f_b} = -\frac{1}{2}N\hat{i} + \left(\frac{\sqrt{3}}{2}N\cos\theta + f\sin\theta\right)\hat{j} + \left(\frac{\sqrt{3}}{2}N\sin\theta - f\cos\theta\right)\hat{k} \tag{9}$$

Since the external force F, and contact forces F_a and F_b in Equations (2), (8), and (9) should be in equilibrium, the following relationships must be satisfied:

$$\begin{cases} \frac{\sqrt{3}}{2}N\cos\theta + f\sin\theta = \frac{1}{2}F_H \\ \frac{\sqrt{3}}{2}N\sin\theta - f\cos\theta = \frac{1}{2}F_v \end{cases} \tag{10}$$

The magnitudes of the local normal force N and friction force f are obtained and expressed in terms of the external vertical force, F_v, and horizontal force, F_H:

$$\begin{cases} N = \frac{\sqrt{3}}{3}(F_H\cos\theta + F_v\sin\theta) \\ f = \frac{1}{2}(F_H\sin\theta - F_v\cos\theta) \end{cases} \tag{11}$$

At the micro-scale, the local normal force N and friction force f can be related to the interparticle friction by:

$$f = N * \tan\phi_\mu \tag{12}$$

where ϕ_μ is the interparticle friction angle.

Substituting N and f from Equation (11) into Equation (12), the interparticle friction can be related to the applied F_v and measured F_H:

$$\tan\phi_\mu = \frac{f}{\mathrm{N}} = \frac{\sqrt{3}}{2} * \frac{F_H\sin\theta - F_v\cos\theta}{F_H\cos\theta + F_v\sin\theta} \tag{13}$$

As indicated in Equation (13), the determination of the interparticle friction angle requires the applied vertical force, F_v, the measured horizontal force, F_H, and the angle θ between the line OA and the xy plane, which can be determined based on the arrangement of the balls.

As shown in Figure 2, the length of OA_{xy} iss equal to $\left(\sqrt{3}/3\right)r$ at the starting point, and then it decreases with the movement of Ball A relative to Balls B and C during the test. By measuring the length of OA_{xy}, the angle θ can be calculated based on the relationship of $\theta = \cos^{-1}\left(OA_{xy}/OA\right)$, where the length of OA is always equal to $\sqrt{3}r$. In addition, the variation of the vertical displacement can be determined by calculating the change in length of AA_{xy}. A sample calculation on the changes in angle θ is provided in Table 1, where ΔOA_{xy} is equal to the change in horizontal displacement and ΔAA_{xy} is equal to the

change in vertical displacement. Both angle θ and vertical displacement increased with the increase in horizontal displacement.

Table 1. The calculated angle θ based on the geometrical relationship.

Horizontal Displacement, ΔOA_{xy}, mm	Angle θ, °	Vertical Displacement, ΔAA_{xy}, mm
0	70.5	0
1	73.3	0.33
2	76.0	0.60
3	78.6	0.83
4	81.3	1.00
$(\sqrt{3}/3)r$	90.0	1.26

4. Experimental Results and Discussion

The experimental results are shown in Figures 5 and 6. Each test was repeated once, which is denoted as Group 1 and Group 2. The results for Group 1 tests are shown in solid lines, and the results of Group 2 tests are shown in dash lines. Figure 5 shows that the horizontal resistance increased with higher confining stresses. The stiffness also increased at higher confining stresses. The difference between the peak horizontal resistance of the two groups of tests under the same normal stress varied from 0.6% to 2.0%. Figure 6 presents the measured vertical displacements versus horizontal displacements. Horizontal displacement was imposed at a fixed rate, and vertical displacement took place while over-riding between the steel balls. It is seen that the vertical displacements are more or less independent of the confining stress. The difference in displacement is about 0.2 mm, which is within the accuracy (i.e., verticality) of the LVDT (Linear Variable Differential Transformer). Both Figures 5 and 6 show that the results are reproducible.

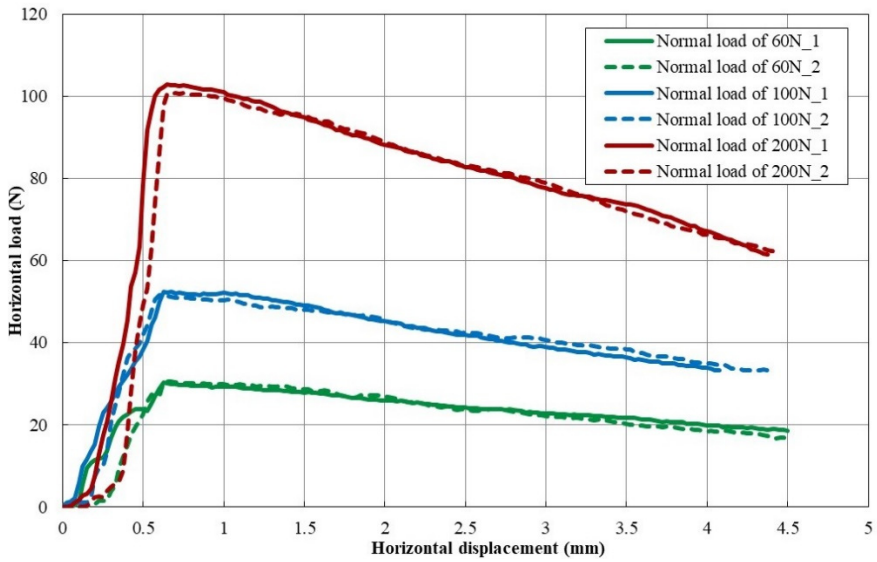

Figure 5. Measured horizontal load versus horizontal displacement for two groups of tests (under normal loads of 60, 100, and 200 N).

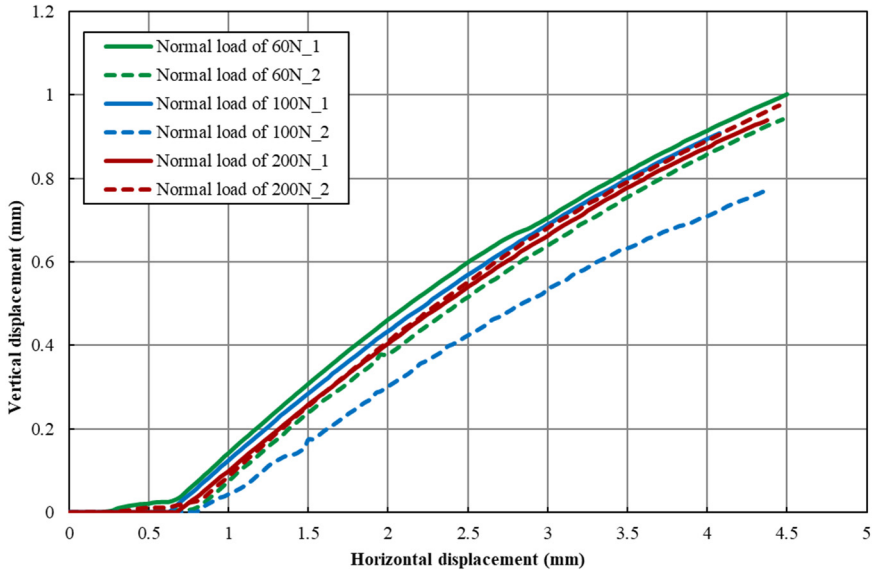

Figure 6. Vertical displacement versus horizontal displacement for two groups of tests (under normal loads of 60, 100, and 200 N).

Based on the test results in Figures 5 and 6, the angle θ in Table 1, and the relationship provided in Equation (13), the interparticle frictions are calculated and summarized in Table 2 for a normal load of 60 N. The friction coefficients of the steel balls' surfaces are between 0.11 and 0.13, with an average value of 0.12. The corresponding interparticle friction angle is about 6.8°. Using a coefficient of friction of 0.12, the horizontal load versus the horizontal displacement curves for vertical normal forces of 100 and 200 N are determined, as shown in Figures 7 and 8, respectively. It can be seen that the theoretical forces and displacement relationships agree well with the experimental measurements. The difference between the theoretical and measured peak horizontal resistance is in the range of 0.2% to 2.6%. The good agreement in peak horizontal forces indicates that the friction angle between the ball surfaces can be measured with reasonable accuracy. The difference between the theoretical and measured horizontal load at small horizontal displacement can be due to the lack of firm contact between the balls at the beginning of the test, and it does not have an impact on the final measurement of the friction angle. Figure 8 shows that the theoretical values match the measured displacement well.

Table 2. The calculated interparticle friction under 60 N normal load.

Vertical Applied Force, N	Interparticle Friction, $\tan\phi_\mu$, at Different Horizontal Displacement				Mean Interparticle Friction Coefficient
	0 mm	1 mm	2 mm	3 mm	
60_1	0.11	0.12	0.12	0.13	0.12
60_2	0.11	0.13	0.11	0.11	

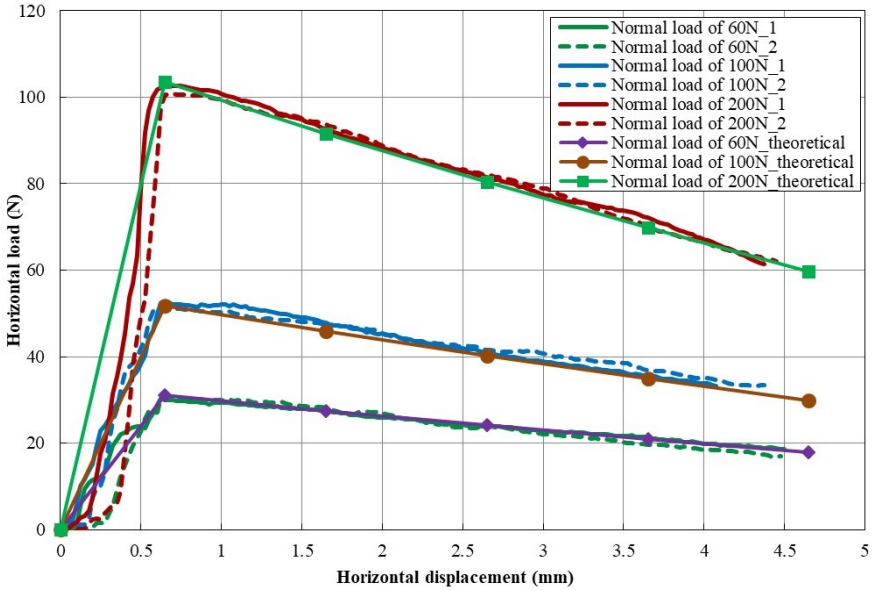

Figure 7. Comparison between measured and calculated horizontal forces based on the measured interparticle friction angle under the normal load of 60 N.

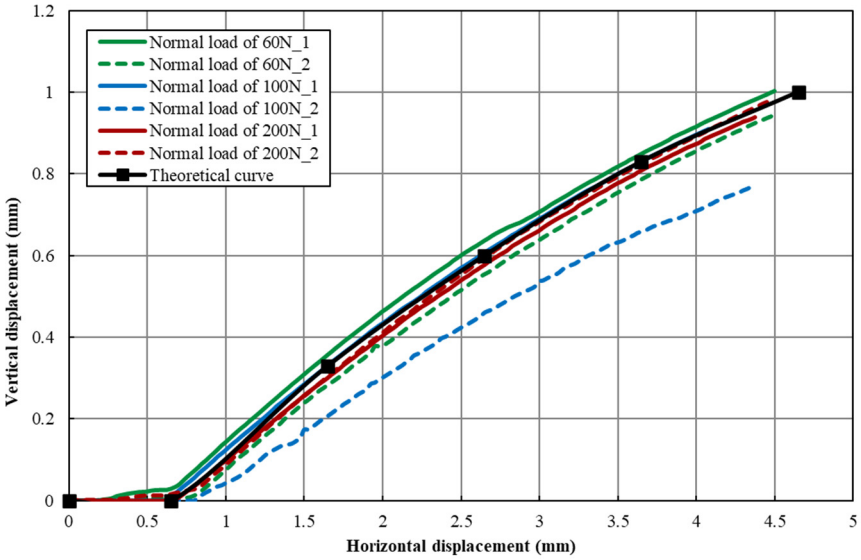

Figure 8. Comparison between measured and calculated vertical displacements based on the measured interparticle friction angle under the normal load of 60 N.

Although the current test apparatus is designed for spherical steel particles, this method can be used for measuring soil particles of reasonable sizes and in the same configuration as presented here. By measuring the horizontal force and vertical/horizontal movements, and with known vertical force, the inclination of movement at the particle contact can be calculated. Based on known vertical and horizontal forces, the shear and normal force on the contact surface can be calculated. By knowing the shear and normal forces on the contact surface, the contact friction can be determined. However, for the case of spherical particles, it is not necessary to use all the measurements to determine the friction since the contact geometry is known, which is the first step for measuring interparticle friction in the laboratory. Further research is needed to extend the measurement technique to particles with other shapes, and eventually irregular shapes.

5. Conclusions

An innovative method is presented here to determine the interparticle friction angle of idealized spherical particles. In this method, a conventional direct shear apparatus can be used to measure the horizontal and vertical forces, which can be used in Equation (13) to estimate the friction angle. The test results are found to be highly reproducible based on duplicated test results from two groups of tests. The method is also shown to be accurate since the theoretical relationship between shear load and shear displacement agree well with experimental measurements.

The apparatus required for this test is readily available in most geotechnical laboratories. The spherical particles are placed in a stable configuration that eliminates the difficulties of particle alignment.

This paper is the first step in developing laboratory techniques for directly measuring interparticle friction. The next step is extending the method to particles with other shapes and, eventually, irregular shapes. The measured friction can then be used in the micromechanical analysis of a wide array of petroleum geomechanics problems, including sanding, wellbore breakouts, and hydraulic fracturing.

Author Contributions: Conceptualization, D.C. and A.N.; Formal analysis, Y.L.; Funding acquisition, A.N.; Investigation, Y.L.; Methodology, D.C.; Resources, D.C. and A.N.; Validation, Y.L.; Visualization, A.N.; Writing—original draft, Y.L.; Writing—review & editing, D.C. and A.N. All authors have read and agreed to the published version of the manuscript.

Funding: This research was funded by NSERC through CRDPJ 387606-09.

Data Availability Statement: Additional information and data can be found at: Li, Y. (2017) Relationship between Micro and Macro Mechanical Properties of Cemented Artificial Conglomerate, PhD thesis, University of Alberta, 2017.

Conflicts of Interest: The authors declare no conflict of interest.

References

1. Procter, D.C.; Barton, R.R. Measurements of the Angle of Interparticle Friction. *Geotechnique* **1974**, *24*, 581–604. [CrossRef]
2. Nascimento, U. Goniometer for Determining Interparticle Friction. In Proceedings of the 9th International Conference on Soil Mechanics and Foundation Engineering, Tokyo, Japan, 10–15 July 1977.
3. Tyrrell, J.W.G.; Cleaver, J.A.S. Development of an Instrument for Measuring Inter-Particle Forces. *Adv. Powder Technol.* **2001**, *12*, 1–15. [CrossRef]
4. Ecke, S.; Raiteri, R.; Bonaccurso, E.; Reiner, C.; Deiseroth, H.; Butt, H. Measuring Normal and Friction Forces Acting on Individual Fine Particles. *Rev. Sci. Instrum.* **2001**, *72*, 4164–4170. [CrossRef]
5. Cavarretta, I.; Rocchi, I.; Coop, M.R. A New Interparticle Friction Apparatus for Granular Materials. *Can. Geotech. J.* **2011**, *48*, 1829–1840. [CrossRef]
6. Senetakis, K.; Coop, M. The Development of a New Micro-Mechanical Inter-Particle Loading Apparatus. *Geotech. Test. J.* **2014**, *37*, 1028–1039. [CrossRef]
7. Sandeep, C.S.; Senetakis, K. An experimental investigation of the microslip displacement of geological materials. *Comput. Geotech.* **2019**, *107*, 55–67. [CrossRef]
8. He, H.; Senetakis, K.; Coop, M.R. An investigation of the effect of shearing velocity on the inter-particle behavior of granular and composite materials with a new micromechanical dynamic testing apparatus. *Tribol. Int.* **2019**, *134*, 252–263. [CrossRef]
9. Jones, R. From Single Particle AFM Studies of Adhesion and Friction to Bulk Flow: Forging the Links. *Granul. Matter* **2003**, *5*, 191–204. [CrossRef]
10. Sandeep, C.S.; Senetakis, K. Micromechanical experiments using a new inter-granule loading apparatus on gravel to ballast-sized materials. *Friction* **2020**, *8*, 70–82. [CrossRef]
11. Muhunthan, B.; Masad, E.; Assaad, A. Measurement of Uniformity and Anisotropy in Granular Materials. *Geotech. Test. J.* **2000**, *23*, 423–431.
12. Nakagawa, S.; Myer, L.R. Mechanical and acoustic properties of weakly cemented granular rocks. In Proceedings of the DC Rocks 2001, The 38th U.S. Symposium on Rock Mechanics (USRMS), Washington, DC, USA, 7–10 July 2001.
13. Akram, M.S. Physical and Numerical Investigation of Conglomeratic Rocks. Ph.D. Thesis, The University of New South Wales, Sydney, NSW, Australia, 2010.
14. Jaafar, R.; Likos, W. Estimating Water Retention Characteristics of Sands from Grain Size Distribution using Idealized Packing Conditions. *Geotech. Test. J.* **2011**, *34*, 489–502.

15. Taslagyan, K.A.; Chan, D.H.; Morgenstern, N.R. Vibrational Fluidization of Granular Media. *Int. J. Geomech.* **2016**, *16*, 04015080. [CrossRef]
16. Rahmati, H.; Nouri, A.; Chan, D.; Vaziri, H. Simulation of Drilling-Induced Compaction Bands Using Discrete Element Method. *Int. J. Numer. Anal. Methods Geomech.* **2014**, *38*, 37–50. [CrossRef]
17. Holt, R.M. Particle vs laboratory modelling of in-situ compaction. *Phys. Chem. Earth* **2001**, *26*, 89–93. [CrossRef]
18. Jiang, M.; Zhang, W.; Sun, Y.; Utili, S. An investigation on loose cemented granular materials via DEM analyses. *Granul. Matter* **2013**, *15*, 65–84. [CrossRef]
19. Fu, Y. Experimental Quantification and DEM Simulation of Macro Behaviors of Granular Materials Using X-ray Tomography Imaging. Ph.D. Thesis, Louisiana State University, Baton Rouge, LA, USA, 2005.
20. Cui, Y.; Nouri, A.; Chan, D.; Rahmati, E. A New Approach to DEM Simulation of Sand Production. *J. Pet. Sci. Eng.* **2016**, *147*, 56–67. [CrossRef]